Preparation of Magnetic Hybrid Copolymer–Cobalt Hierarchical Hollow Spheres by Localized Ostwald Ripening

Ru Qiao, Xiao Li Zhang, Ri Qiu, Ju Chang Kim, and Young Soo Kang*

Department of Chemistry, Pukyong National University, 599-1 Daeyeon-3-dong, Namgu, Busan 608-737, Korea

Received July 18, 2007. Revised Manuscript Received October 12, 2007

We report a one-step solvothermal method to prepare magnetic hybrid copolymer–Co hierarchical hollow spheres by localized Ostwald ripening. The initial stage is the aggregation of primary inorganic nanoparticles whose surfaces are partially adsorbed by copolymer PEG–PPG–PEG to form solid spheres followed by hollowing of the core and the progressive matter redistribution from the interior to the exterior. Meanwhile, amorphous inorganic particles grow to cubic crystallites. Finally, a hollow spherical architecture with an extensively roughened surface is obtained by this self-transformation. The effect of NaOH concentration (served as a catalyst and reagent) on the sphere morphology is also checked by time-dependent experiments. When decreasing the mass of NaOH from 7.5 to 2.5 mmol, a morphology transformation from porous hollow spheres to double-wall spheres and then to single-wall spheres with platelet-like building units aligned disorderly on the outer surfaces is observed, and this morphology transformation is related to Ostwald ripening. Our results suggest that these nanoparticle-based hollow hierarchical spheres collected by the self-transformation of precursor objects could be of potential applicability in the fields of material science and biomedical technology.

Introduction

The unique physicochemical properties displayed by hollow structures have received increasing attention in the past few years, especially assembly of inorganic components into polymeric hollow spheres is of particular interest due to combination of the properties of inorganic and organic components, thereby making them ideal candidates for applications ranging from targeting drug delivery, catalysis carriers, isolated chemical reactors, to bioseparation.[1,2] There have been two main categories of preparative methods: (1) the template-directed synthesis and (2) the emulsion synthesis.[3–7] However, all of these methods are labor-intensive processes, in which preparation of template, coating of the template with a shell, and removal of the template to create the hollow core are successively conducted. Especially, removal of the templates after synthesis utilizing separation methods such as base etching and calcinations may sometimes damage the desired configurations of the hollow spheres which result in structure collapse.[8] To further simplify the synthetic process of these interesting hollow spheres, it is essential to devise a new way to do it. In our previous work, we have already demonstrated that hybrid hollow microspheres formed by self-assembly of Co magnetic nanoparticles (NPs) and block copolymer PEG–PPG–PEG, which not only affords protective coatings to prevent oxidation of Co particles but also gives the product an advantage for excellent dispersibility in most polar and nonpolar solvents, could be obtained through a facile one-step solvothermal route, without templates in ethylene glycol solvent.[9] This solvothermal approach endues the hybrid hollow spheres with a thermal stability, and it is easy to scale up for industrial need. The hybrid microspheres with both advantages of the biocompatible amphiphilic property of the block copolymer and the superparamagnetic property of Co particles make these products have potential applications as multifunctional directed materials in the fields of material science and biotechnology.

In the current report, we describe a further discussion about the formation mechanism of polymeric Co hollow spheres in the solvothermal process. On the basis of initial reports by Fievet and co-workers,[10,11] it can be confirmed that the formation of primary Co nanoparticles in ethylene glycol depends on a polyol process. The polyol synthesis has been known as a simple and versatile method for producing metal nanoparticles, in which a diol or polyalcohol (such as

* Corresponding author. E-mail: yskang@pknu.ac.kr.

(1) (a) Meier, W. *Chem. Soc. Rev.* **2000**, *29*, 295. (b) Caruso, F. *Adv. Mater.* **2001**, *13*, 11. (c) Yu, A.; Wang, Y.; Barlow, E.; Caruso, F. *Adv. Mater.* **2005**, *17*, 1737.
(2) (a) Zhong, Z.; Yin, Y.; Gates, B.; Xia, Y. *Adv. Mater.* **2000**, *12*, 206. (b) Lacík, I.; Briššová, M.; Anilkumar, A. V.; Powers, A. C.; Wang, T. *J. Biomed. Mater. Res.* **1998**, *39*, 52. (c) Briššová, M.; Lacík, I.; Powers, A. C.; Anilkumar, A. V.; Wang, T. *J. Biomed. Mater. Res.* **1998**, *39*, 61.
(3) Caruso, F.; Caruso, R. A.; Möhwald, H. *Science* **1998**, *282*, 1111.
(4) Dhas, N. A.; Suslick, K. S. *J. Am. Chem. Soc.* **2005**, *127*, 2368.
(5) Chen, M.; Wu, L. M.; Zhou, S. X.; You, B. *Adv. Mater.* **2006**, *18*, 801.
(6) Wang, P.; Chen, D.; Tang, F. Q. *Langmuir* **2006**, *22*, 4832.
(7) (a) Yang, Z.; Niu, Z.; Lu, Y.; Hu, Z.; Han, C. C. *Angew. Chem., Int. Ed.* **2003**, *42*, 1943. (b) Sun, Q. Y.; Kooyman, P. J.; Grossmann, J. G.; Bomans, P. H. H.; Frederik, P. M.; Magusin, P. C. M. M.; Beelen, T. P. M.; Santen, R. A. V.; Sommerdijk, N. A. J. M. *Adv. Mater.* **2003**, *15*, 1097.
(8) (a) Li, X. H.; Zhang, D. H.; Chen, J. S. *J. Am. Chem. Soc.* **2006**, *128*, 8382. (b) Li, B.; Rong, G.; Xie, Y.; Huang, L.; Feng, C. *Inorg. Chem.* **2006**, *45*, 6404.
(9) Qiao, R.; Zhang, X. L.; Qiu, R.; Li, Y.; Kang, Y. S. *J. Phys. Chem. C* **2007**, *111*, 2426.

10.1021/cm701904x CCC: $37.00
Published on Web 11/20/2007

Table 1. Experimental Conditions for Typical Co/Copolymer Hybrid Product and Their Morphologies[a]

sample	solution	time (h)	morphology
1	EG(40 mL)/2 mmol of $CoCl_2 \cdot 6H_2O$, 0.35 mmol of PEG–PPG–PEG/7.5 mmol of NaOH	15	hollow spheres with the extensively roughened surface
2	same as sample 1	3	nanoparticles
3	same as sample 1	5	solid spheres
4	same as sample 1	12	hollow spheres
5	2.5 mmol of NaOH; other term same as before	12	porous hollow spheres
6	same as sample 5	13	double-wall structure
7	same as sample 5	15	single-wall spheres with platelet-like building units aligned on the outer surface
8	same as sample 5	6	mixture of submicroparticles and hollow spheres
9	same as sample 5	9	nondense hollow spheres

[a] All samples were prepared by the solvothermal method at 200 °C.

ethylene glycol, diethylene glycol,[12] triethylene glycol, or tetraethylene glycol) is used as both solvent and reducing agent. Although the mechanism of this reaction is still poorly understood, it has been confirmed the reduction is based on the decomposition of the ethylene glycol and its conversion to diacetyl,[13] and then it is followed by the multistep aggregation of the amorphous inorganic particles that are partially stabilized by surface-adsorbed block copolymers. When a longer reaction time is provided, the aggregated precursor microspheres will undergo self-transformation such that hollow interiors can be further created via localized Ostwald ripening, a traditional physical phenomenon, within metastable solid microspheres.[14,15]

As part of our continuing work on the hybrid hollow microspheres formed by self-assembly of Co magnetic NPs and block copolymer PEG–PPG–PEG,[9] herein we report that, by simply decreasing the catalyst (NaOH) concentration, the novel hierarchical architectures of block copolymer–Co magnetic NPs hybrid microspheres with hollow interior features are obtained at different reaction times; at first, the primary Co magnetic NPs coated by PEG–PPG–PEG aggregate together to form 3D porous microspheres with a void core. With increasing the reaction time, the magnetic NPs located on the outermost surface would serve as starting points to attract the small particles underneath for the subsequent crystallization process, which result in the void space between the loosely packed exterior and the closely packed interior and the formation of double-wall hollow spheres. Once the cores in the center are consumed completely, the final single-wall hollow spheres will be created, and the platelet-like building units align on the outer side of their shells. The succession of morphology transformations obtained by time-dependent experiments after decreasing alkali content has been rarely reported in the literature before. It can be explained by the Ostwald ripening growth mechanism.[16–21] We expect that these novel architecture systems are potentially important for utilizations such as interesting candidates for optical, sensing, electronic, and drug-delivery application. However, we focus on the preparation and the formation mechanism of these interesting products here.

Experimental Section

All the chemical reagents were of analytical grade and used without further purification.

Synthesis. Block copolymer–Co MPs hybrid hollow spheres were synthesized through a simple solvothermal reaction according to a previous report.[9] In a typical procedure, 2 mmol of cobaltous chloride hexahydrate ($CoCl_2 \cdot 6H_2O$), poly(ethylene glycol)-*block*-poly(propylene glycol)-*block*-poly(ethylene glycol) (PEG–PPG–PEG, M_n = 2800, Aldrich), and 7.5–2.5 mmol of NaOH were dissolved in 40 mL of ethylene glycol (EG, 99.5%, Aldrich). The mixture was then put into a Teflon-lined stainless steel autoclave of 50 mL capacity. The sealed tank was heated at a rate of 15 °C/min to 200 °C and maintained at this temperature for different reaction times ranging from 3 to 15 h in an oven. After reaction, the autoclave was cooled to room temperature naturally. The resulting precipitates were washed with anhydrous ethanol several times to remove the residual reagents. The samples used for characterization were dispersed in ethanol and were ultrasonicated before FESEM and TEM observation. The experimental conditions for typical hybrid products and their final morphologies are listed in Table 1. Samples 1 and 8 were also dried and calcinated in N_2 at 400 °C for 2 h to obtain bare inorganic cobalt products by decomposing organic composition.

Characterization. The crystallinity of the synthesized polymeric cobalt hybrid spheres was characterized using an X-ray diffractometer (X′Pert-MPD, Philips) with Cu Kα radiation. The XPS spectrum for hybrid copolymer–Co products was acquired using a Thermo VG Scientific Multilab 2000 system equipped with a Mg Kα X-ray source at 1253.60 eV. The FT-IR spectrum was recorded in KBr on an FT-IR spectrometer (Perkin-Elmer) at wavenumbers

(10) Figlarz, M.; Fievet, F.; Lagier, J. P. U.S. Patent Pat. No. 4,539,041, 1985.
(11) Fievet, F.; Lagier, J. P.; Figlarz, M. *MRS Bull.* **1989**, *14*, 29.
(12) Martorana, B.; Carotenuto, G.; Pullini, D.; Zvezdin, K.; Peruta, G. L.; Perlo, P.; Nicolais, L. *Sens. Actuators, A* **2006**, *129*, 176.
(13) Kerner, R.; Palchik, O.; Gedanken, A. *Chem. Mater.* **2001**, *13*, 1413.
(14) Yu, J.; Guo, H.; Davis, S. A.; Mann, S. *Adv. Funct. Mater.* **2006**, *16*, 2035.
(15) (a) Yu, S.-H.; Cölfen, H.; Antonietti, M. *J. Phys. Chem. B* **2003**, *107*, 7396. (b) Yu, S.-H.; Cölfen, H. *J. Mater. Chem.* **2004**, *14*, 2124.
(16) Yang, H. G.; Zeng, H. C. *Angew. Chem., Int. Ed.* **2004**, *43*, 5206.
(17) Liu, B.; Zeng, H. C. *Small* **2005**, *1*, 566.
(18) (a) Zheng, Y.; Cheng, Y.; Wang, Y.; Zhou, L.; Bao, F.; Jia, C. *J. Phys. Chem. B* **2006**, *110*, 8284. (b) Cheng, Y.; Wang, Y.; Jia, C.; Bao, F. *J. Phys. Chem. B* **2006**, *110*, 24399.
(19) (a) Chang, Y.; Teo, J. J.; Zeng, H. C. *Langmuir* **2005**, *21*, 1074. (b) Yang, H. G.; Zeng, H. C. *J. Phys. Chem. B* **2004**, *108*, 3492.
(20) (a) Luo, C.; Xue, D. *Langmuir* **2006**, *22*, 9914. (b) Xu, J.; Xue, D. *J. Solid State Chem.* **2007**, *180*, 128.
(21) Wang, W. S.; Zhen, L.; Xu, C. Y.; Zhang, B. Y.; Shao, W. Z. *J. Phys. Chem. B* **2006**, *110*, 23154.

of 4000–400 cm^{-1}. The microstructure of produced spheres was studied by a field-emission scanning electron microscope (FESEM, JEOL JSM-6700F) and a transmission electron microscope (TEM, JEOL JEM-100). Compositional information of the specimens was analyzed using energy-dispersive X-ray spectroscopy (EDX). Thermogravimetric analysis measurement was performed with a thermal analyzer (TGA-7, Perkin-Elmer) under a nitrogen atmosphere at a temperature range of 50–600 °C; the heating rate was 10 °C/min. A Quantum Design Magnetometer (MPMS XL 7) using a superconducting quantum interference device (SQUID) sensor was used to make measurements of the specific magnetization of the hybrid spheres in applied magnetic fields over the range from −10 000 to +10 000 Oe at 5–300 K.

Results and Discussion

The essence of polyol synthesis is the reduction of a metal salt by EG at high temperatures in the presence of NaOH. First, metal hydroxide is produced and followed by the precipitation of the intermediate phase and its progressive dissolution. In the second step, the dissolved intermediate phase is reduced in EG solvent to form metal particles.[10,11,22] The general mechanism of metallic cobalt can be represented by the following three proposed steps:

$$2HOCH_2CH_2OH \rightarrow 2CH_3CHO + 2H_2O \quad (1)$$

$$Co^{2+} + 2OH^- \rightarrow Co(OH)_2 \quad (2)$$

$$Co(OH)_2 + 2CH_3CHO \rightarrow CH_3COOCCH_3 + Co + 2H_2O \quad (3)$$

At the same time, the long polymeric chain structure of PEG–PPG–PEG can be adsorbed on the surface of one or more nanoparticles. It is followed by the self-assembly of Co magnetic NPs and copolymer PEG–PPG–PEG into the hybrid hollow microspheres.

Hybrid copolymer–Co hollow spheres were prepared by treatment of a mixture of cobaltous chloride hexahydrate, EG, NaOH, and PEG–PPG–PEG at 200 °C for 15 h (sample 1 in Table 1). Although shells of the products are too thick to get TEM images testifying the interior structure, the collapsed and broken structures in FESEM images can clearly show that the obtained microspheres are hollow, and the external surfaces of the shell walls are extensively roughened (Figure 1). Particle size distributions show a relatively uniform size population with mean diameter of 4.1 ± 0.8 μm. The inset of Figure 1b illustrates the XRD pattern of the hybrid products. The discernible peaks can be indexed to (111), (200), and (220) planes, which correspond to those of the cubic structure of cobalt (JCPDS card file no. 15-0806). The crystal sizes determined by the Scherrer equation with XRD data have been calculated to be 15 nm, which indicates that metallic cobalt in hybrid products is nanocrystalline. The magnetization curve measured at room

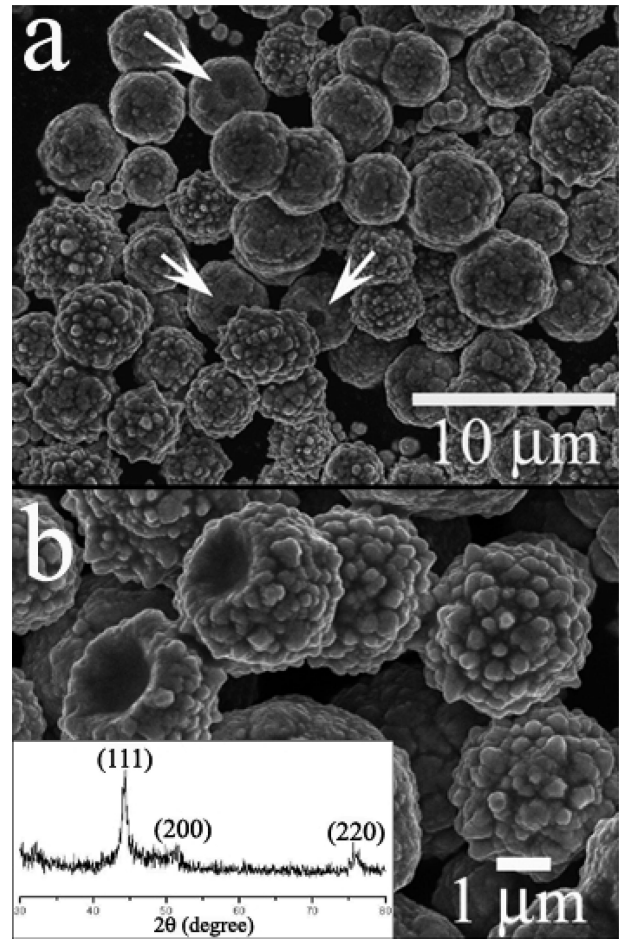

Figure 1. (a) Low- and (b) high-magnification FESEM images of copolymer–Co hollow spheres obtained from sample 1. Inset in (b) is the XRD pattern of these products.

temperature of sample 1 is shown in Figure S1. The good overlap of the curve is consistent with the superparamagnetic response. The X-ray photoelectron spectrum of the hybrid products shows the binding energy of the Co $2p_{3/2}$ main line at 781.9 eV (Figure 2a). At 787.3 eV binding energy there is a satellite peak. The binding energy of the Co $2p_{3/2}$ (781.9 eV) cannot be ascribed to CoO (780.1 eV) or $Co(OH)_2$ (780.9 eV) but could be related to the effect of the adsorption of organic components on these inorganic NPs. Similar results have been reported by Corma and co-workers that cobalt metallic particles in an inorganic framework show high binding energy (782.1 eV).[23] To further confirm the uniqueness of Co NPs, the crystal structure and composition of the calcinated sample 1 were examined by XRD and EDX. The XRD pattern in Figure S2 shows the residual inorganic products after calcinations are in accordance with cobalt JCPDS card no. 01-1255 and no. 01-1259. A typical EDX spectrum is presented in Figure 2b. The spectrum confirms that the crystals are composed only of Co. The Au signals come from the Au film. They also help us to ensure the absence of CoO or $Co(OH)_2$ in our sample.

For a complete view of the formation process of hybrid copolymer–Co hollow spheres and their growth mechanism,

(22) (a) Xiong, Y.; Mclellan, J. M.; Chen, J.; Yin, Y.; Li, Z. Y.; Xia, Y. *J. Am. Chem. Soc.* **2005**, *127*, 17118. (b) Komarneni, S.; Li, D.; Newalkar, B.; Katsuki, H.; Bhalla, A. S. *Langmuir* **2002**, *18*, 5959.

(23) Barea, E.; Batlle, X.; Bourges, P.; Corma, A.; Fornés, V.; Labarta, A.; Puntes, V. F. *J. Am. Chem. Soc.* **2005**, *127*, 18026.

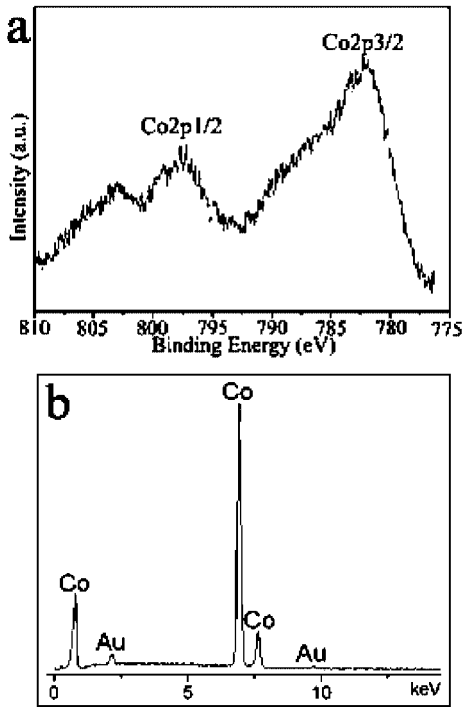

Figure 2. (a) XPS spectrum obtained from the hybrid copolymer–Co hollow spheres (sample 1). (b) EDX spectrum obtained from the calcinated sample 1.

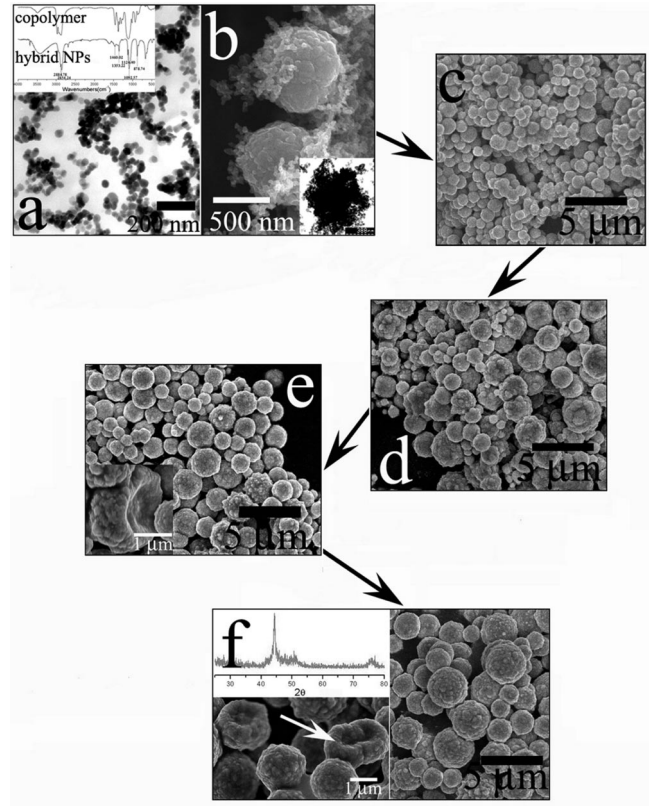

Figure 3. (a, b) TEM and FESEM images of products respectively collected after 3 h of reaction. Insets of (a) and (b) show the FTIR spectrum of the hybrid NPs and TEM image of aggregated submicrospheres, respectively. (c, d, e) FESEM images of products obtained after 4, 5, and 6 h of reaction, respectively. Inset of (e) shows the collapsed structure of a hollow sphere. (f) XRD pattern and FESEM images of hollow spheres produced after 12 h of reaction.

detailed time-dependent evolutions of morphology and crystallinity at 200 °C were elucidated by TEM, FESEM, and XRD analysis, which are shown in Figure 3. As shown in Figure 3a, samples collected after 3 h of reaction time consisted of hybrid nanoparticles in which metallic particles were amorphous structure (XRD data not shown). Proof of the copolymer component of the products was provided by the FTIR spectrum, as presented in the inset of Figure 3a, where the typical PEG–PPG–PEG absorption bands at 1092.57, 1353.22, 1460.02, 2854.24, and 3419.46 can be clearly seen. At this stage, the higher local concentration of inorganic particles caused their self-aggregation followed by the formation of solid submicrospheres with a narrow particle size distribution (Figure 3b). This kind of uniform submicrosphere can be obtained in large quantities by limiting the reaction time as 4 h (Figure 3c). The similar formation of spherical aggregation of polymer-protected magnetite has been established by Hou et al.[24,25] Extending the reaction time to 5 h resulted in ununiformed microspheres with a rough surface. The progressive increase in the particle size was due to the secondary aggregation of the submicrospheres (Figure 3d). Interestingly, as shown in Figure 3e and its inset, the inorganic nanoparticles located in the inner cores began to dissolve because of the higher surface energies, and a hollowing effect was observed when providing an additional 1 h of reaction. If 12 h of reaction was applied, XRD profile indicated that the inorganic components in hybrid products grew to cubic crystal structure, and the average crystal size was about 11.4 nm. Figure 3f indicates that a peanut-shaped structure existed in this process. Compared with the final products obtained after 15 h of reaction (Figure 1), it could be confirmed that these peanut-shaped dimers were just a kind of intermediate product which was formed between two tightly connected neighboring hollow spheres. As a result, the larger hollow spherical architectures were created through absorption and integration between the two.

It is believed that localized Ostwald ripening should be the main driving force for this self-transformation. The ripening process has been commonly observed in general crystal growth for more than one century, and it involves "the growth of larger crystals from those of smaller size which have a higher solubility than the larger ones".[26] Such ripening processes have been discussed in detail for preparation of TiO_2 and Cu_2O hollow spheres in Zeng's previous work.[18] On the basis of the above evolution of the time-dependent experiments, this process was associated with a progressive redistribution of matter from the interior to the exterior of the microspheres.[13,18] It is characterized by the initial deposition of amorphous solid spheres. The amorphous core remains out of equilibrium with the surrounding solution due to its high solubility so that it dissolves and undergoes diffusion. As a consequence, the supersaturation increases

(24) (a) Hou, Y.; Gao, S.; Ohta, T.; Kondoh, H. *Eur. J. Inorg. Chem.* **2004**, 1169. (b) Hou, Y.; Kondoh, H.; Ohta, T. *Chem. Mater.* **2005**, *17*, 3994.
(25) Hou, Y.; Kondoh, H.; Shimojo, M.; Sako, E. O.; Ozaki, N.; Kogure, T.; Ohta, T. *J. Phys. Chem. B* **2005**, *109*, 4845.
(26) Ostwald, W. *Z. Phys. Chem.* **1900**, *34*, 495.

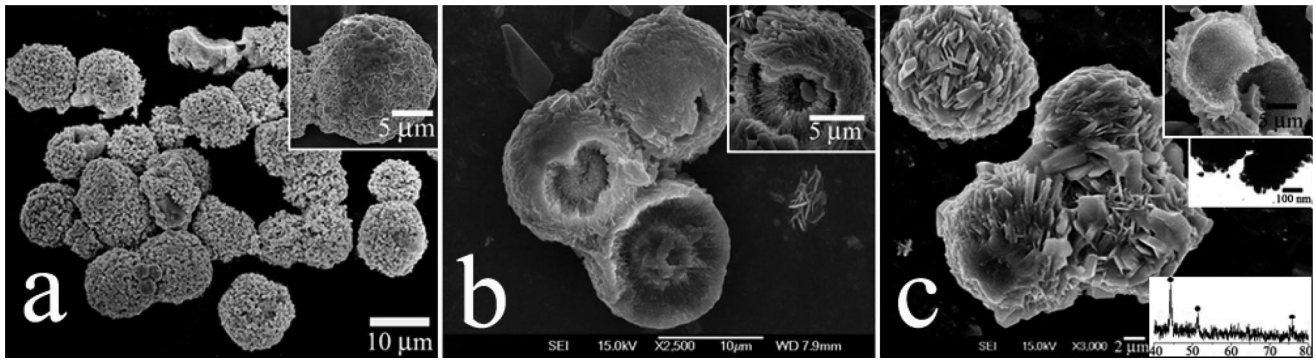

Figure 4. FESEM images of hybrid hollow spheres obtained with 2.5 mmol of NaOH in reaction systems and after different reaction times: (a) 12 h, showing porous hollow spheres (inset: a magnified image); (b) 13 h, showing hollow spheres with double-wall structures (inset: the typical image of a fractured sphere); (c) 15 h, showing hollow spheres with platelet-like building units aligned on the outer surface (inset: FESEM image of fractured spheres, TEM image of building units, and XRD pattern).

above the solubility product of the exterior layer in the solution which results in secondary deposition of inorganic products on the exterior surface. Thus, the particle size distribution increases as the core dissolves progressively to produce hollow spheres. And it can be confirmed that, when remaining at constant temperature, this self-transformation is strongly dependent on reaction time.

Here, NaOH was used as a catalyst and reagent. To investigate the influence of NaOH on the formation process of these hollow amphiphilic magnetic spheres, a controlled experiment was carried out under the different NaOH concentration. It is found that, as shown in Figure 4a, when the content of NaOH is decreased from 7.5 to 2.5 mmol (sample 5, Table 1), the hollow spheres with a rough surface are replaced by the ones with a porous structural feature after 12 h of reaction, which are formed by aggregation of the primary nanoparticles, and the XRD pattern indicates an amorphous structure (data not shown). The particle size of the products was also increased to about 10 ± 1 μm. Therefore, according to the above-mentioned results, it indicates that, when all other conditions remain the same as sample 4, reducing the content of NaOH could result in a larger porous spherical structure, and its effect on Co particles is that the inorganic nanoparticles is changed to amorphous structure. So, the content of NaOH affects the formation time of the Co crystallites in the hybrid spheres and the morphology of the shell wall.

To obtain a better understanding of the evolution of hybrid copolymer–Co hollow spheres after decreasing the content of NaOH, a series of time-dependent experiments, in which the reactive reagents were the same as sample 5, were also carried out. The shape evolution at the middle reaction time of spherical growth (sample 6, Table 1) is shown in Figure 4b. It is interesting that new double-wall core–shell structures are observed after 13 h of reaction, and the inorganic components are still the amorphous structure here. When the reaction is prolonged to 15 h, the cores in the center of core–shell spheres have vanished at this stage, and platelet-like building units can be observed on the outer surface of the shell (sample 7, Table 1). It is because that, with the reaction continuing, the concentration of reactants decreases; an oriented dissolving step of inorganic nanoparticles occurs subsequently to form the platelet-like building units for

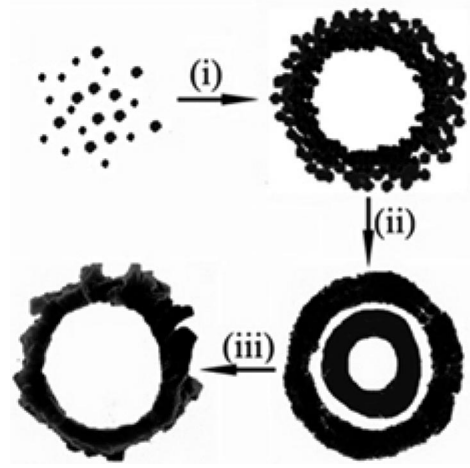

Figure 5. Schematic illustration of the morphology transformation of copolymer–Co hybrid spheres via localized Ostwald ripening.

eliminating the higher surface energy faces. Finally, the complete evacuation of the cores in the center of core–shell spheres results in the single-wall hollow structure, as displayed in Figure 4c. The XRD pattern in Figure 4c indicates a clear crystalline structure of Co nanoparticles. Using the Scherrer equation for an estimation of progressive crystallite growth, it is found that the mean size of the crystallites formed in this process is 23 nm, which agrees with the actual crystallite sizes of the nanoparticles observed by TEM (inset of Figure 4c).

On the basis of the above results, it is believed that Ostwald ripening process continues to play a major role in the formation of these novel hierarchical architectures. A schematic representation is shown in Figure 5. The formation and evolution of microspheres seem to be as follows: In the initial stage, driven by the minimization of the total energy of the system, the primary PEG–PPG–PEG copolymer-coated Co colloids are aggregated together with a nondense hollow spherical appearance. This primary stage has been an approved byproduct of samples 8 and 9. Sub-microparticles and hollow spheres with a large scale visibly coexist after 6 h of reaction (sample 8), as shown in Figure S3a. After calcinating the composites at 400 °C for 2 h, the residual inorganic parts are confirmed to be Co crystals with hexagonal structure (inset of Figure S3a, JCPDS card file no. 05-0727). Interestingly, nondense hollow spheres can be

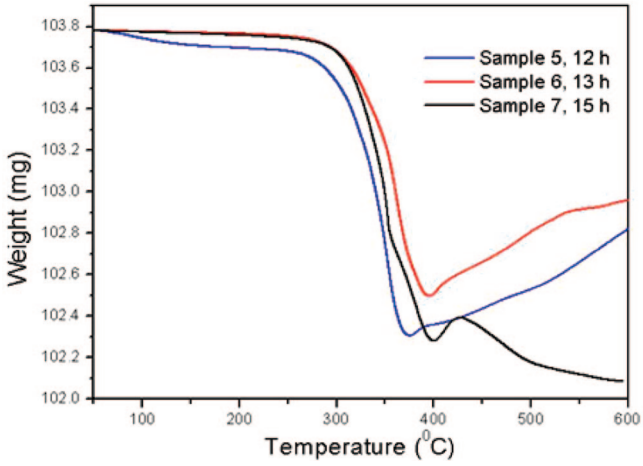

Figure 6. TGA curves of the hierarchical products obtained from samples 5–7.

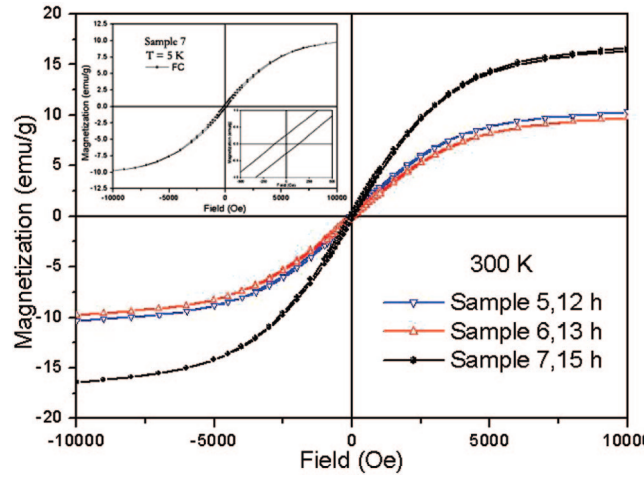

Figure 7. Magnetization curves of the hierarchical products obtained from samples 5–7 measured at 300 K. Inset: the hysteresis loop of sample 7 at 5 K after a field cooling in a field magnetization of 10 000 Oe and its expanded plot for field strengths between −500 and 500 Oe.

obtained when increasing the reaction time up to 9 h (Figure S3b, sample 9). And then, we got the porous hollow spheres, in which the interior particles packed more closely than the exterior ones (Figure 5i), after 12 h of reaction because of the absorption between inorganic particles. With the reaction continuing, the concentration of reactants decreases and the reaction rate slows down. The exterior particles packed loosely would serve as starting points on attracting the smaller amorphous particles underneath for the subsequent recrystallization process, while new depositions grow on the edge renewedly, which leads to the initial formation of platelet-like building units on the outer surface. As the mass is transported, the void space between the exterior loosely packed areas and the interior closely packed ones is generated mainly through the symmetric ripening, which results in double-wall hollow spheres (Figure 5ii). With increasing reaction time to 15 h, inorganic nanoparticles are grown from amorphous structure to cubic structure, indicating that the crystallinity of inorganic particles increases. And at this stage, the cores in the center of the spheres are consumed completely, so the final single-wall hollow spheres are created (Figure 5iii). As shown in Figure 4c, the fractured spheres reveal that the building units grow much larger with the depositions of the crystallites dissolved into the solution and align disorderly on the outer surface of the shell. Therefore, the current experiments indicate that Ostwald ripening is an underlying mechanism in this hollowing process.

Thermogravimetric analysis (TGA) of hybrid copolymer–Co products obtained from samples 5–7 reveals the presence of PEG–PPG–PEG copolymer (Figure 6). There is a phenomenon of reincrease in mass for samples above 400 °C. It is deduced that cobalt oxides were formed by the reaction between bare cobalt NPs and decomposition products of copolymer. The reason for reincrease in mass for sample 7 may arise from the decomposition of a trace of impurity. The effect on mass ratio can be ignored. The magnetic properties of these obtained products shown in Figure 7 are determined by the superconducting quantum interference device (SQUID) magnetometer. Almost undetectable hysteresis and coercivity suggest that these hybrid products have nearly superparamagnetic properties at room temperature. As shown in TGA curves, the total weight losses of these three samples are very close, so we can propose that the mass ratios of inorganic/organic components in these samples are approximately equal, and the saturation magnetization of sample 7 increases to 16.4 emu g^{-1} at room temperature only because of the growth of the Co crystallites. Compared with the saturation magnetization of the bulk Co metal (164 emu g^{-1}),[27] it is still much lower; the reduction in the magnetic value of our produced materials can be attributed to the small particle size effect[28,29] and the quantities of nonmagnetic organic components. Although the hybrid spheres exhibit relatively low magnetization, a clear magnetic response is evident and can readily be used in some fields of materials which require low magnetic property.

The inset of Figure 7 shows the hysteresis loop of sample 7 at 5 K after a field cooling (FC) in a field magnetization of 10 000 Oe. The FC loop displays an expected ferromagnetic behavior at low temperature, and it is symmetrical in shape around the origin which clearly reveals the nonexistence of unidirectional exchange anisotropy of cobalt oxide impurity.[30,31]

Conclusions

In the present work, various hierarchical architectures of PEG–PPG–PEG copolymer–Co hybrid hollow spheres were synthesized through a solvothermal method. It has been demonstrated that localized Ostwald ripening plays a major role in formation of these novel hollow structures. The process was associated with a progressive redistribu-

(27) (a) Pauthenet, R. *J. Appl. Phys.* **1982**, *53*, 8187. (b) Grass, R. N.; Stark, W. J. *J. Mater. Chem.* **2006**, *16*, 1825.
(28) Shafi, K. V. P. M.; Gedanken, A.; Goldfarb, R. B.; Felner, I. *J. Appl. Phys.* **1997**, *81*, 6901.
(29) Shafi, K. V. P. M.; Ulman, A.; Dyal, A.; Yan, X.; Yang, N. L.; Estournès, C.; Fournès, L.; Wattiaux, A.; White, H.; Rafailovich, M. *Chem. Mater.* **2002**, *14*, 1778.
(30) Peng, D. L.; Sumiyama, K.; Hihara, T.; Yamamuro, S.; Konno, T. J. *Phys. Rev. B* **2000**, *61*, 3103.
(31) Verelst, M.; Ely, T. O.; Amiens, C.; Snoeck, E.; Lecante, P.; Mosset, A.; Respaud, M.; Broto, J. M.; Chaudret, B. *Chem. Mater.* **1999**, *11*, 2702.

tion of matter from the interior to the exterior and the crystal growth of inorganic components. On the basis of their amphiphilic and magnetic properties, we expect that these versatile targeting hollow spheres could be of great potential in the field of biotechnology or as carriers.

Acknowledgment. This work is financially supported by a Korea Research Foundation Grant for foreign graduate student, Brain Korea 21 program, and the nano R&D program (Korea Science & Engineering Foundation, Grant 2007-02628).

Supporting Information Available: Magnetization curve of sample 1, XRD obtained from the calcinated sample 1, and FESEM images of samples 8 and 9. This information is available free of charge via the Internet at http://pubs.acs.org.

CM701904X